Vacuum-ultraviolet absorption bands of trivalent lanthanides in LaF_3†

Wm. S. Heaps,* L. R. Elias,‡ and W. M. Yen
Department of Physics, University of Wisconsin, Madison, Wisconsin 53706
(Received 11 November 1974)

The ultraviolet absorption bands of trivalent rare earths in LaF_3 are located by the use of absorption and selective excitation spectra. These absorptions are quite strong arising from the electric dipole transition, which promotes a $4f$ electron from the rare-earth $4f^n$ shell to the $5d$ or some higher-lying orbital. The onsets of the $5d$ absorptions range from about 40000 cm^{-1} for cerium to beyond 80000 cm^{-1} for lutetium showing a general increase from cerium to gadolinium, a sudden drop from gadolinium to terbium, and another increase. The positions of the bands are compared with estimates by several workers of the $5d$ level position for trivalent free ions. In general the LaF_3 crystal field lowers and broadens the $5d$ level with respect to its free-ion counterpart. For the simplest rare earth, cerium, the splitting caused by the LaF_3 crystal field is calculated using a point-charge model. Agreement with experiment is poor, so a two-parameter fit to the splitting is made which indicates that the point-charge model plus the approximation for the radial integrals involved overestimate the crystal-field perturbation on the $5d$ electron by roughly a factor of 3.

I. INTRODUCTION

In this paper we present the results of a comprehensive study of the uv properties of lanthanides doped into LaF_3. For the most part the uv absorption in these materials derives from transitions involving the promotion of an electron from the $4f$ shell to the $5d$ or a higher-lying shell. These are allowed electric dipole transitions. Consequently the absorption is quite strong. Historically the spectra of rare earths in solids could be characterized as consisting of many sharp lines in the visible and infrared which had no counterparts in the free-ion spectra. These lines are now known to arise from transitions within the $4f^n$ manifold occurring via an electric dipole mechanism. The crystal field mixes states of opposite parity with the $4f^n$ states permitting electric dipole transitions. In solids for which the ion site symmetry is too high (inversion symmetry is present) no sharp lines are seen. The optically active $4f$ electrons interact only weakly with the host crystal ions because the $4f$ electrons are screened from the crystalline environment by the $5s$ and $5p$ electrons of the rare-earth ion, these orbits have greater radii than that of the $4f$ orbit. This characteristic is responsible for the sharpness of the observed lines. It also causes the rare earths to behave similarly chemically making the production of pure samples difficult.

The main thrust of the theoretical treatment of rare-earth ions has been the analysis of the $4f^n$ configuration. These problems are quite complex in that the large number of electrons with large angular momentum combine to create a vast number of states. Sophisticated mathematical techniques have been developed which render these problems manageable. The shielding of the $4f$ electrons from the crystal field reduces its effect to the extent that calculations for free-ion energy levels agree well with those observed in solids. Other configurations have not received as much attention. The calculation of the energy levels of higher configurations in solids is extremely difficult. As with the $4f^n$ configuration, many states are involved but the mathematical techniques for treating these configurations are not as fully developed. The promoted electron lies beyond the shielding $5s$ and $5p$ orbitals where it can interact strongly with the lattice ions. Only a few cases have been treated, and these are the simplest ions in crystal fields of high symmetry. Several empirical analyses of higher configurations do exist and comparison will be made between these and our data.

Experimental work on the higher configurations has been hindered by the fact that most of the transitions occur in the vacuum uv region of the spectrum. The use of synchrotron radiation from an electron storage ring allows one to surmount many of the traditional experimental difficulties facing the spectroscopist working in this region. It is also noteworthy that this work encompasses two types of spectra, absorption and selective excitation, which complementing one another allow a much more confident determination of the uv properties of the rare earths.

II. THEORY

The majority of the theoretical work on lanthanide energy levels has concerned itself with the $4f^n$ configuration. Although the techniques for calculating these levels has been available in prin-

ciple for a long time, the extreme complexity of the systems involved (3432 states for $4f^{14}$) hindered the emergence of energy-level schemes.[1] Many results were forthcoming in the 1960's owing to the application of the digital computer and Racah's methods developed two decades earlier.[2-4] Recent developments of schemes for classifying states promise to ease the calculational difficulties involved still further.[5]

Energy-level calculations for higher configurations of the free ion are available. Judd[6] has worked out the general case for configurations of the form $l^n l'$ on the assumption that spin-orbit effects are stronger for the single electron than are electrostatic effects between it and the electrons in the other orbit (j-j coupling).[7] An analogous model could be developed for ions in crystals since the single electron would couple to the lattice much more strongly than the remaining electrons.

Another approach to the analysis of the spectra can be found in the works of Brewer, Martin, Sugar, and Reader,[8-10] in which regularities in the existing data are used to predict as yet unmeasured features. Their work is relatively successful in providing the values of interest for most of the ions. Our results have shown that the locations of bands in crystals are considerably affected by temperature and concentration, hence precision of greater than a few thousand wave numbers is unnecessary.[11] No analysis of the empirical type exists for ions in solids, but they may appear as more experimental data becomes available.

III. EXPERIMENTAL DETAILS

All spectra were taken using synchrotron radiation from the University of Wisconsin Physical Sciences Laboratory electron storage ring. The storage ring operates at 240 MeV at a frequency of about 32 MHz. Beam currents ranged from 1–20 mA. The radiation is a continuum peaked at about 500 Å and extending well into the visible. The highly relativistic electron bunch emits the light in a forward peaked cone and polarized horizontally. Because the light originates in a vacuum the uv may impinge directly on the sample under study with no unwanted absorption from windows or atmosphere complicating the results.

A. Absorption

Figure 1 is a diagram of the experimental apparatus for absorption. Light from the storage ring was collected by elliptical mirrors and focussed on the entrance slit of a $\frac{1}{2}$-m McPherson scanning monochromator. The grating was blazed

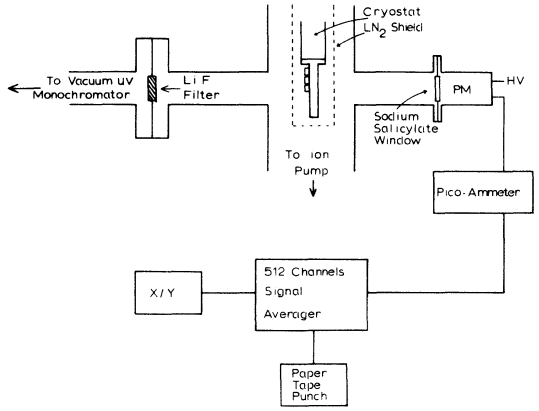

FIG. 1. Diagram of the experimental arrangement for the absorption studies. For the excitation spectra a quartz window mounted on the side was used with either a filter or monochromator for wavelength selection.

at 1200 Å and was overcoated with an Al-MgF_2 film to increase its reflectivity. From the monochromator the light passed through a filter of LiF or suprasil quartz and struck the sample. The filters limited the light to first order for ranges of 1040–2000 and 1800–3000 Å, respectively.

The samples were provided by W. Hargreaves of Optovac. The LaF_3 matrix had a purity of 99.999% and the dopant had a purity of 99.99%. During the experiment we noted considerable absorption and fluorescence by impurities other than that specified. Praseodymium and cerium were present in practically every sample. This is not surprising considering the large oscillator strength of the transitions involved plus the possibility of 0.001 mol.% contaminant. The samples were cut and polished into 10×1-mm disks, with the c axis in the plane of the disk. They were mounted on a cold finger tip with GE 7031 varnish. Sample temperature was monitored with a Au-Cu thermocouple. The signal was detected by a photomultiplier tube (EMI 9558Q) attached to a quartz window lined with sodium salicylate. Sodium salicylate absorbs over a wide range in the uv and fluoresces at 4000 Å. The signal from the photomultiplier tube was amplified by a Keithley model 417 pico-ammeter and stored in the first half of the memory of a Nuclear Data Enhancetron. The storage-ring beam current was sampled during the scan and stored in the second half of the Enhancetron memory. This permitted point by point normalization of the transmission data against the exponentially decaying beam current. The Enhancetron memory was stored permanently on paper tape for subsequent digital processing. Traces were also taken with no sample to permit normalization of the data to the passband of the LiF or suprasil filter.

B. Selective excitation

The excitation spectra were taken using the Pruett-Lien normal incidence monochromator which was designed and built by the Physical Sciences Laboratory staff. This monochromator is a horizontally dispersing, 1-m instrument with grating blazed at 700 Å. The 0.75-mm slits we employed gave a resolution of 6.25 Å. Light from the monochromator illuminated the samples which were attached to the same liquid-N_2 cold finger. A few of the samples used for selective excitation were rectangular (7×7×10 mm) with the c axis parallel to one of the edges. These too were obtained from Optovac.

Fluorescence from the samples was observed at 90° to the exciting beam in a horizontal plane. The light passed through a sapphire window and was focussed by a quartz lens onto the entrance slit of a Jarrel-Ash $\frac{1}{4}$-m monochromator. In some cases a Corning 3-72 filter was placed between the window and the lens to eliminate second-order radiation. Fluorescence intensity was monitored directly with a photomultiplier tube (EMI 9558Q) cooled with vapor from liquid N_2. In a few cases a narrow-band filter replaced the quartz lens and monochromator assembly. The rest of the apparatus was the same as that used for absorption. Since no LiF or suprasil filter was used for these experiments higher orders of radiation from the monochromator were also incident upon the sample. To insure that these higher orders were not responsible for the fluorescence scans beginning at 0 Å were made for every sample.

IV. RESULTS

Our results can be viewed from two perspectives: that of examining each ion in turn or that of examining the whole lanthanide series for trends. This section consists of a detailed examination of the spectra for each ion. The free-ion calculations mentioned are from Sugar and Reader.[10] The trends of the whole series will be described in the following section.

A. Cerium ($4f^1$)

The ground configuration of the free cerium ion consists of but two ^2F levels separated by 2253 cm^{-1}.[12] The infrared spectrum of this ion in LaF_3 has been determined by Buchanan, Rast, and Caspars,[13] who located all but the highest level of the $^2F_{5/2}$ state. The uv spectrum of CaF_2:Ce^{3+} has been investigated by Loh[14] and more recently by Manthey[15] and by Szczurek, Drake, and Schlesinger.[16] The $5d$ configuration has a $^2D_{3/2}$ state at 497 47 cm^{-1} and a $^2D_{5/2}$ at 522 26 cm^{-1}

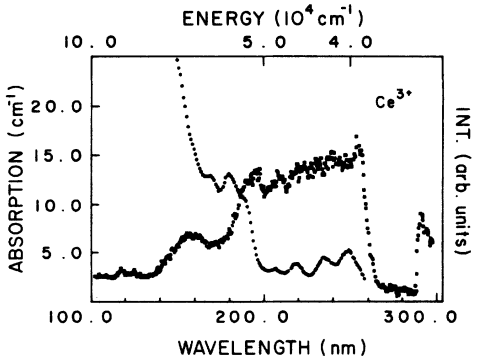

FIG. 2. The trace which rises at high energy is absorption for a 0.01-mol.% sample of cerium. The excitation spectrum is a 5% sample. The rise at 295 nm is scattered light. Note the small bump at 120 nm.

above the ground state. Figure 2 gives an absorption trace for a 0.01-mol.% sample at 100°K and a selective excitation trace of a 5-mol.% sample taken at 3040 Å. The peaks in absorption between 1600 and 1950 Å arise from Pr^{3+} impurities which were present in most samples. The 3040-Å fluorescence is a broad one arising from the relaxation of the $5d$ electron back to the ground state.[17] Note that the Pr^{3+} bands are not seen here. As previously noted the actual extend of the bands is quite dependent upon concentration and temperature but the $5d$ configuration may be said to lie between 1800 and 2600 Å. The $6s$ is between 1400 and 1800 Å. Note that the photon energies giving rise to the band denoted $6s$ are capable of inducing a variety of absorption mechanisms (e.g., charge transfer). The name $6s$ will be retained for convenience but should not necessarily be considered the true identity of the absorption. The lowering of the $5d$ configuration (~10000 cm^{-1}) arises from the host crystal field

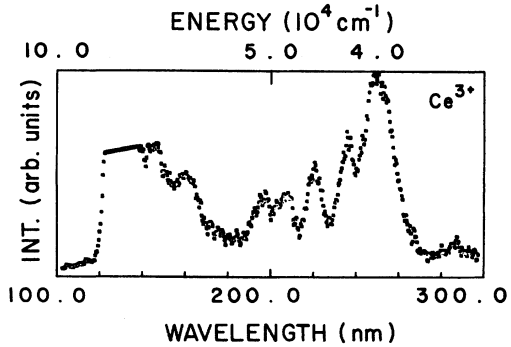

FIG. 3. Excitation spectrum taken at 300 nm for a sample of 1% Tm^{3+}. This spectrum is due to trace cerium in the sample and shows all five energy levels of the $5d$ electron. The 120-nm peak here is large but has been clipped by the enhancetron memory.

and the spin-orbit splitting. The free-ion spin-orbit splitting is about 2500 cm^{-1}. We therefore expect that the crystal field is responsible for most of the splitting of this configuration. The site symmetry at the position of the Ce^{3+} ion has been determined to be C_2.[18] Under this symmetry the $5d$ band must split into five components. Four of these may be resolved from the absorption trace but the excitation spectrum is incapable of resolving these components. Figure 3 is an excitation spectrum of a 1-mol.% sample of Tm^{3+} taken at 2880 Å. These peaks are certainly the $5d$ components of Ce^{3+} which appears as a trace impurity in this sample, and their positions may be determined to be 1871, 2103, 2206, 2353, and 2500 Å.

One other interesting feature may be noted in the cerium traces. This is a peak at 1190 Å below the cutoff for LaF_3. In Fig. 2 the peak may just be resolved about 400 Å below the $6s$ peak. In Fig. 3 and several traces at various concentrations not shown it is more evident. In fact the same peak is comparable in size to the cerium $5d$ peaks. There are two possibilities for the identity of this peak. It may be caused by an impurity which has a $5d$ absorption here and fluoresces in the region 2900–3100 Å. Or it may involve absorption of the uv by some impurity with subsequent transfer of the excitation to the cerium ion. Spectra of the fluorescence from 2700 to 3300 Å were taken while exciting the sample with 1190-Å light. An impurity fluorescence should be much narrower than the Ce^{3+} fluorescence because it arises within the $4f^n$ configuration. Unfortunately the light levels were so low that an unambiguous determination of the fluorescence linewidth could not be made. We were pleased to note that the selective excitation method appeared capable of allowing examination of the ion absorption somewhat below the LaF_3 cutoff frequency.

B. Praseodymium ($4f^2$)

The free trivalent ion of praseodymium has been studied in detail by Crosswhite *et al.*[19] and Sugar.[20] The $4f5d$ configuration occurs between 61 170 and 78 776 cm^{-1}. The $4f6s$ lies at about 100 000 cm^{-1}. Figure 4 gives an absorption spectrum and a selective excitation spectrum for a 0.01-mol.% sample. The sharp rise at about 2000 Å is the onset of the $4f^2 \rightarrow 4f5d$ absorption band. The increase at 1400 Å is the $6s$ band absorption. The $4f^2$ configuration of Pr^{3+} consists of 13 energy multiplets the highest of which, $^1S_0$, is very near the $4f5d$ levels. Carnall *et al.*[21] have investigated several crystal matrices and

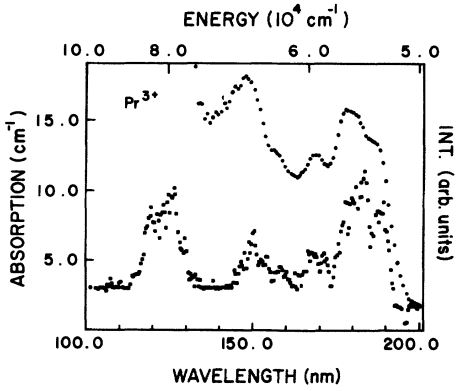

FIG. 4. Absorption and excitation traces for 0.01-mol.% sample of praseodymium. In all the following traces that which rises at short wavelengths is absorption unless otherwise noted.

reports that for all but LaF_3 the $^1S_0$ level lies within the $4f5d$ band. The proximity of this level to the band (3000 cm^{-1}) allows high population of this level via the $5d$ and $6s$ bands. We have reported previously on the many strong uv and visible fluorescence lines resulting from population of the $^1S_0$ state. Using one of these ($^1S_0 \rightarrow {}^1I_6$) it was possible to take the excitation spectrum of Pr^{3+} shown in Fig. 4. Although the structure of the bands cannot be completely resolved, these two spectra allow us to locate the $4f5d$ band in the range 1950–1450 Å (51 300–69 000 cm^{-1}). The $4f6s$ level begins at about 1330 Å (75 000 cm^{-1}) but its full extent is obscured by the onset of LaF_3 absorption. As with cerium the exact location of these bands varies slightly with temperature and concentration. The depression of the configurations (~10 000 cm^{-1} for $4f5d$; 25 000 cm^{-1} for $4f6s$) from the free-ion values is caused by the LaF_3 crystal field. The exact analysis of these configurations is made more complex than for cerium by the presence of the Coulomb repulsion term. Praseodymium was found as an impurity in almost every other sample that we had. Its absorptions made interpretation of other absorption spectra difficult. Likewise the strong fluorescence lines originating on the $^1S_0$ state necessitated caution in taking the selective excitation spectra.

C. Neodymium ($4f^3$)

Neodymium is the most abundant and most thoroughly studied of the lanthanides. The $4f^3$ configuration for the ion in LaF_3 was investigated by Caspers.[22] The free-ion $5d$ band begins at 70 100 cm^{-1}, the $6s$ band at 108 900 cm^{-1}. Figure 5 is an absorption trace of 0.01-mol.% Nd^{3+} and a selective excitation spectrum of 1-mol.% Nd^{3+} monitored at 2190 Å. We have not identified the

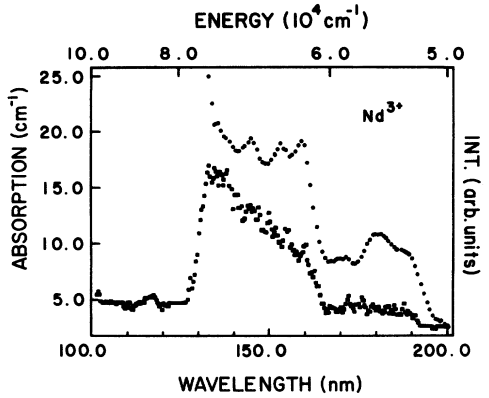

FIG. 5. Absorption and excitation traces for a 0.01-mol.% and a 1-mol.% sample of neodymium, respectively. Both traces show evidence of praseodymium impurity.

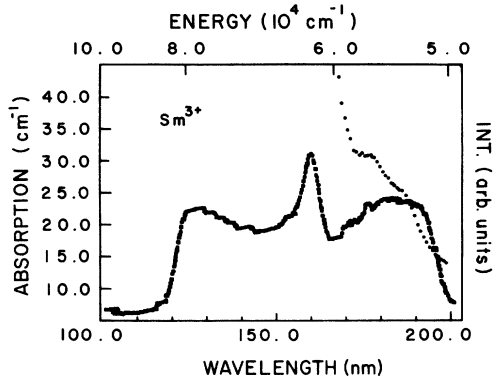

FIG. 6. Absorption and excitation traces for a 0.01-mol.% and a 1-mol.% sample of samarium. Again both traces show some praseodymium impurity.

transition responsible for this fluorescence. The excellent correspondence of the structure of the trace with that of the absorption trace and with excitation spectra taken monitoring other fluorescence lines in Nd lead us to believe that it is indeed a Nd^{3+} fluorescence arising from a $5d$-$4f$ transition. Other possibilities are transitions originating on the $^2F_{7/2}$, $^2G_{9/2}$, or $^2G_{7/2}$ levels.[23] The smaller structure on the excitation trace is most probably Pr^{3+} which has a fluorescence near 2190 Å. With the reminder that this too is sensitive to temperature and concentration we put the $5d$ band for Nd^{3+} in the range 61 000 and 76 000 cm^{-1}. The $6s$ band apparently lies well beyond the LaF_3 cutoff.

D. Promethium ($4f^4$)

Promethium is highly radioactive, artificial, and expensive. We had no LaF_3:Pm^{3+} samples. The $4f^4$ configuration in $LaCl_3$ has been investigated recently.[24] The free-ion calculation puts the $5d$ band at 73 300 cm^{-1} and the $4s$ band at 111 000 cm^{-1}.

E. Samarium ($4f^5$)

The ground configuration of trivalent samarium in LaF_3 has been investigated by Rast, Fry, and Caspars.[25] The $4f^5$ configuration consists of 73 multiplets. Under the perturbations of spin-orbit, crystal field, and magnetic fields those multiplets can split into 2002 states. Consequently even for the ground configuration the spectra are exceedingly complex. Figure 6 gives an absorption trace of a 0.01-mol.% sample of Sm^{3+} and an excitation spectrum monitored at 5600 Å. This fluorescence arises from the transitions from the $^4G_{5/2}$ level within the $4f^5$ manifold and is quite strong. Both traces indicate that the $5d$ band begins at about 58 000 cm^{-1} and extends well beyond the LaF_3 cutoff. The presence of Pr^{3+} absorption on the excitation trace is evidence for activation of the Sm^{3+} fluorescence by Pr^{3+}. In samples with higher concentration this type of mechanism is quite probable.

F. Europium ($4f^6$)

Our europium sample was contaminated by the divalent ion. Figure 7 is an absorption spectrum of 0.01-mol.% europium in LaF_3. The strong absorption is most probably the $4f^6 \rightarrow 4f^5 5d$ transition for the divalent ion. The free divalent ion $5d$ level is calculated to begin at 33 900 cm^{-1} and the $6s$ level at 44 300 cm^{-1}.[10] No excitation spectra were taken for this ion.

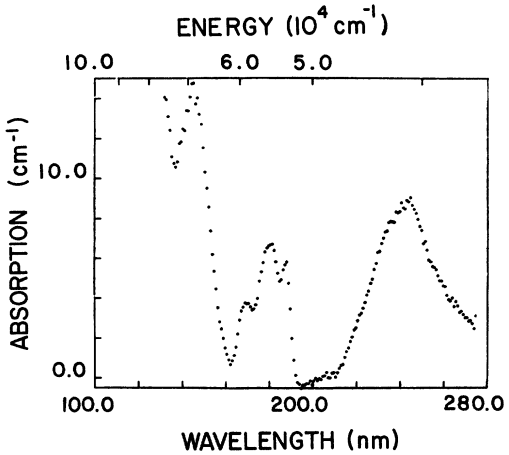

FIG. 7. Absorption trace of a 0.01-mol.% sample of europium. The low-energy absorption is caused by the divalent ion $4f - 5d$ transition. Praseodymium is also evident as an impurity.

G. Gadolinium ($4f^7$)

The ground configuration of trivalent gadolinium in LaF_3 has been investigated by Carnall, Fields, and Sarup.[26] The lowest excited state of Gd^{3+}, the $^6P_{7/2}$ level, lies 32 176 cm^{-1} above the ground $^8S_{7/2}$ state. Crosswhite and Kielkopf[27] have studied the free-ion spectrum and have identified several lines from the $4f^6 5d$ configuration occurring between 104 000 and 122 000 cm^{-1}.[28] We were unable to observe any absorption in LaF_3:Gd^{3+} directly, presumably because the LaF_3 and impurity absorption masked that of the gadolinium. Figure 8 is an excitation spectrum of a 1-mol.% sample of Gd monitored at 3140 Å. Here we can see the onset of the $5d$ absorption at about 77 000 cm^{-1}. The small bump around 60 000 cm^{-1} is most probably the cerium $6s$ absorption since cerium also fluoresces at 3140 Å. The gadolinium absorption is probably responsible for the unexplained feature in the cerium excitation spectra.

H. Terbium ($4f^8$)

The terbium ground configuration has a very complicated spectrum which has not been completely analyzed above 26 000 cm^{-1}. Dieke indicates that the $4f^7 5d$ configuration is split and of great extent for the free ion.[28] Figure 9 gives an absorption and excitation spectrum for a 0.1-mol.% sample of LaF_3: Tb^{3+}. The fluorescence monitored for the excitation spectrum arises from transitions from the $^5D_3$ level. Agreement between the traces is good except that the gap so evident in the excitation spectrum is less prominent for the absorption. It may be masked by impurity absorption. We believe the gap is genuine and corresponds to the split predicted by Dieke.

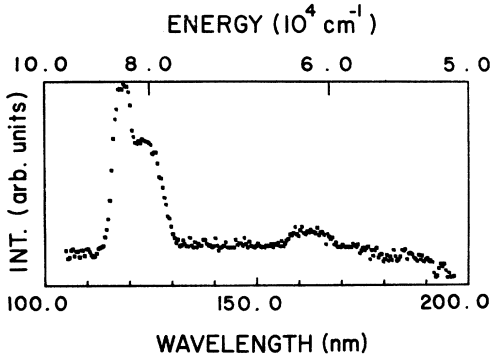

FIG. 8. Selective excitation trace of a 1-mol.% sample gadolinium. Because it fluoresces in the same region as cerium, gadolinium is a possible source of the spurious 120-nm band in the cerium traces.

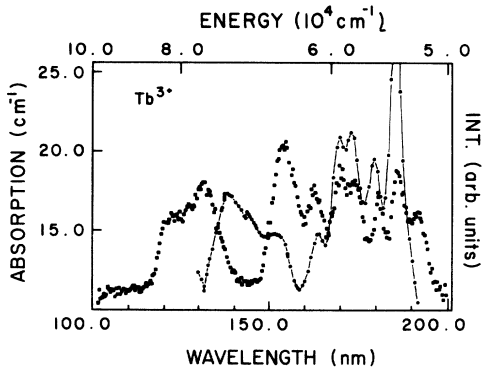

FIG. 9. Absorption trace and excitation trace for a 0.1-mol.% sample of terbium. (The connected dots are absorption.) The discrepancy near 150.0 nm is probably caused by impurity absorption.

I. Dysprosium ($4f^9$)

The ground configuration of trivalent dysprosium in LaF_3 has been investigated by Fry, Caspars, Rast and Miller.[29] The spectrum here is very complex and an accurate assignment of states has not been made above 24 000 cm^{-1}. The free-ion calculation gives a value of 66 300 cm^{-1} for the onset of the $5d$ band and 99 100 cm^{-1} for the $6s$ level. Figure 10 shows absorption and excitation spectra for a 0.5-mol.% sample. The 5730-Å fluorescence monitored for the excitation spectrum arises from a $^4F_{9/2}$-$^6H_{13/2}$ transition within the $4f^9$ configuration. Both the traces show an absorption beginning at about 60 000 cm^{-1} and extending beyond the LaF_3 cutoff.

J. Holmium ($4f^{10}$)

The spectrum of trivalent holmium is sufficiently simple that virtually complete energy-level

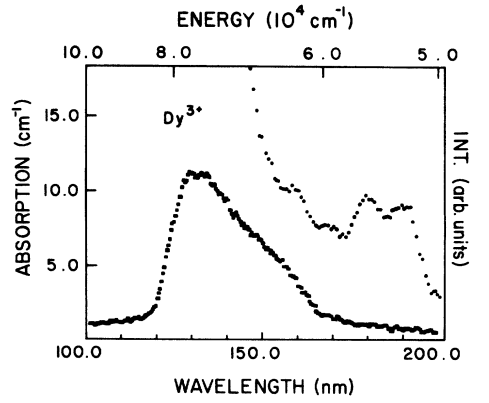

FIG. 10. Absorption trace and an excitation trace for a 0.5-mol.% sample of dysprosium. The absorption trace shows considerable impurity absorption.

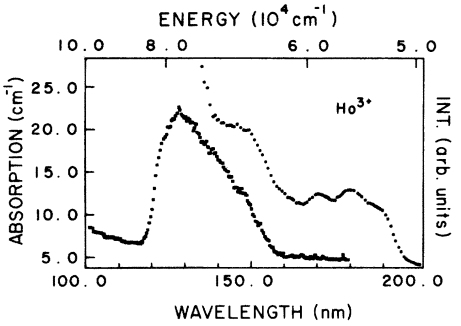

FIG. 11. Absorption trace and an excitation trace for a 0.01- and a 1-mol.% sample of holmium, respectively. The absorption trace shows impurities.

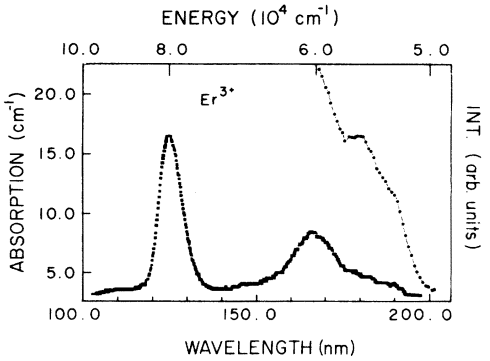

FIG. 12. Absorption trace and an excitation trace for a 0.01-mol.% sample of erbium. The origin of the large peak at 125.0 nm is not yet known.

diagrams for the ground configuration have been obtained for a variety of crystalling hosts. Fry, Caspers, and Rast have examined LaF_3:Ho^{3+} and report complete level assignments up to 26 000 cm^{-1} through absorption and fluorescence spectra.[30] The free-ion calculation puts the 5*d* band beginning at 74 200 cm^{-1} and the 6*s* at 104 000 cm^{-1}. Figure 11 is an absorption spectrum for a 0.01-mol.% sample and an excitation spectrum for a 1-mol.% sample. The 5360-Å line monitored for the excitation spectrum arises from a $^5S_2$-$^5I_8$ transition within the $4f^{10}$ manifold. Both traces show an absorption beginning about 64 500 cm^{-1} and extending beyond the LaF_3 cutoff.

K. Erbium ($4f^{11}$)

The energy levels of the ground configuration of Er^{3+} are well known up to 25 000 cm^{-1} from extensive studies of the ion in $LaCl_3$.[31-33] Krupke and Gruber have examined the ion in LaF_3.[34] The free-ion calcuation of Sugar and Reader locates the onset of the 5*d* absorption at 75 400 cm^{-1} and that of the 6*s* band at 103 600 cm^{-1}. Figure 12 presents an absorption and an excitation spectrum for a 0.01-mol.% sample. The fluorescence for the excitation spectrum arises from the transition of the $4f^{11}$ configuration. The absorption trace shows two shoulders. The first appears to be the familiar Pr^{3+} absorption. The second at 58 000 cm^{-1} appears to be the erbium 5*d* absorption onset. The excitation trace also shows an absorption beginning at 58 000 cm^{-1} as well as some Pr^{3+} absorption observed by the fluorescence of Pr^{3+} which also occurs within the passband. The larger peak at 80 000 cm^{-1} is not identified yet; it may be praseodymium 6*s* absorption.

L. Thulium ($4f^{12}$)

The ground configuration of Tm^{3+} in LaF_3 has been investigated by Carnall *et al.*[35] who succeeded in locating every excited state of the configuration except $^1S_0$ which lies far in the vacuum uv. The free-ion estimate puts the 5*d* onset at 74 300 cm^{-1} and the 6*s* at 101 300 cm^{-1}. Figure 13 gives an absorption trace of a 0.01-mol.% sample and an excitation spectrum of a 1-mol.% sample. The fluorescence for the excitation spectrum probably arises from a 5*d* band transition to the ground configuration. The absence of structure on the excitation trace is rather puzzling and the gradual rise of the absorption makes exact location of the onset difficult. If one assumes that the structure on the absorption trace is caused by unwanted impurities then 70 000 cm^{-1} appears to be a good value from the excitation spectrum but does not seem to fit in well with the levels observed for other ions.

M. Ytterbium ($4f^{13}$)

Ytterbium has no fluorescence in the near uv or visible which could be monitored for an ex-

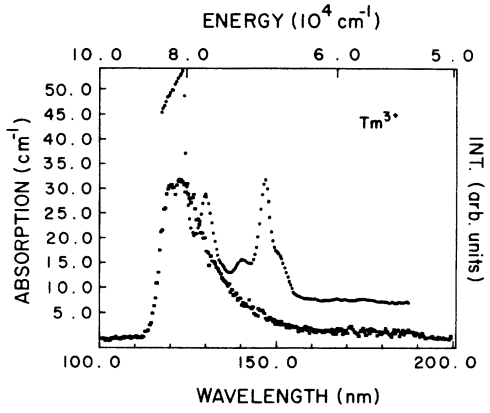

FIG. 13. Absorption trace and an excitation trace for a 0.01- and a 1-mol.% sample of thulium, respectively. It is believed that the structure on the absorption trace is caused by other impurities.

citation spectrum. Absorption traces failed to locate any feature ascribable to Yb^{3+}. We presume that the entire absorption band for Yb^{3+} was masked by impurity absorption. The estimates for the free ion are 80200 and 107500 cm^{-1} for the $5d$ and $6s$ onsets, respectively.

N. Lutetium

Likewise no data could be gathered for lutetium. The free-ion $5d$ onset has been measured to be 90433 cm^{-1} and the 6_s onset is 116798cm^{-1}.[36]

V. ANALYSIS

The exact theoretical treatment of the energy-level problem for the $5d$ configuration of each ion in LaF_3 does not appear to be a worthwhile problem. This can readily be seen. The site symmetry of a rare-earth ion in LaF_3 is very low (C_2) so the crystal field for a d electron requires eight parameters for its characterization.[18] In order to evaluate these from the data one must resolve and identify at least nine lines within the configuration. The number of lines in the configuration increases rapidly towards the center of the series (5 for Ce^{3+}, 140 for Pr^{3+}); but broadening processes in the crystal eliminate the possibility of resolving and identifying specific lines within this configuration in most instances. As a consequence attempts to evaluate the crystal-field parameters by fitting an experiment are destined for failure. However if one knows the radial wave functions for the ion in question, then the crystal-field perturbation can be calculated directly and the energy levels can be compared with experimental values. As an example of this procedure this calculation has been carried out for the simplest ion—Ce^{3+}.

The location of ions in LaF_3 is given in Ref. 18. There are three distinct sites for the fluorine ion in the crystal. The lanthanum ions are all in sites of equivalent symmetry but the axes of the symmetry are 120° apart in the hexagonal plane. The unit cell contains 6 lanthanum ions and 18 fluorine ions. We begin by expressing the crystal potential as a series in spherical harmonics. We are free to choose our coordinate system so we pick one in which the origin lies on a lanthanum site. The z direction corresponds to the axis of symmetry of the ion and the x direction corresponds to the c axis of the crystal. The expression for A_n^m, the expansion coefficient for the spherical harmonics, is

$$A_n^m = \sum_i \left(\frac{4\pi}{2n+1}\right)\left(\frac{qi}{r_i^{n+1}}\right) Y_n^{-m}(\theta_i, \phi_i),$$

where the sum is over all the ions in the crystal.

In order to evaluate these constants a computer program was written to add up the contributions to A_n^m from each ion in the unit cell. The program then displaces the unit cell by one lattice constant and calculates the contribution from the displaced unit cell. It was found that for unit cells more than seven lattice constants away from the origin the contribution to A_n^m was negligible. The results of this calculation, which includes the contribution from every ion within a parallelopiped fourteen lattice constants on a side centered at the origin, are given in Table I. It must be remarked that these constants have been calculated in the point-charge model which treats each ion in the lattice as if it were a point charge. This model neglects several effects which have been shown to be important in crystal-field calculations. First of all it neglects the effect of induced multipoles on each ion. That is to say, the crystal field acting on the ions in the lattice induce higher moments in the charge distribution of the ion. Second, if one is dealing with $4f$ or $5f$ electrons, this model neglects the effect of screening by the electrons in orbitals of greater radius than the $5f$ or $4f$ electron. (The $5s$ and $5p$ electrons in the case of the lanthanides.) Finally, the model neglects the effects of covalency, which is to say that the overlap of the electrons wave function of the central ion and those of its nearest neighbors affect the charge distribution considerably—particularly for those ions which contribute most to A_n^m.[37]

Nevertheless we are ready now to calculate the matrix elements for the crystal-field perturbation matrix. The wave functions that we need for cerium are relatively simple single-electron wave functions. We use the prescription for constructing trial wave functions given in Griffith

TABLE I. LaF_3 crystal-field coefficients in the point-charge model.[a]

Parameter	Real part	Imaginary part
A_2^0	−2060	0.0
$A^{\pm 2}$	−1816	±2347
A_4^0	−155.6	0.0
$A_4^{\pm 2}$	60.80	∓83.65
$A_4^{\pm 4}$	−47.81	±32.39
A_6^0	−3.559	0.0
$A_6^{\pm 2}$	−8.845	∓2.188
$A_6^{\pm 4}$	3.83	∓1.918
$A_6^{\pm 6}$	6.446	±2.422

[a] See Ref. 37.

TABLE II. Crystal-field perturbation matrix for a single $5d$ electron using the values from Table I.

−2072	0	159.9 $-i313.2$	0	−3030 $-i2053$
0	322.5	0	−10 820 $+i13\,776$	0
159.9 $+i313.2$	0	−5777	0	159.9 $-i313.2$
0	−10 820 $-i13\,776$	0	322.5	0
−3030 $+i2053$	0	159.9 $+i313.2$	0	−2072

and attributable to Slater.[38] These have the form

$$\varphi = r^{n^*-1}\exp[-(z-\sigma)r/n^*a]\,Y_1^m,$$

where $n^* = 1, 2, 3, 3.7, 4, 4.2$ for $n = 1, 2, 3, 4, 5, 6$, respectively. z is the atomic number of the ion, σ is a sum of values for each electron in the ion, and a is the Bohr radius.

The angular parts of the integrals are readily performed being simply products of three spherical harmonics. Many elements vanish including all the A_6 terms. The radial part of the matrix may be evaluated either analytically or numerically. Once this is done we obtain the matrix presented in Table II. The eigenvalue problem is then solved for this matrix with the results presented in Table III. The poor agreement between the theoretical and experimental values could come about from a variety of causes. The neglect of co-valency and the roughness of the radial wave functions are probably the most severe causes of the discrepency with neglect of the spin-orbit interaction of secondary importance.

Since the calculation from first principles of the energy levels was not particularly effective it was thought that perhaps the alternative of treating the crystal-field coefficients as parameters and fitting these to the data might offer some insight into the physical situation. We are still faced with the problem of too many parameters for the number of observations. We do know that the A_6 matrix elements vanish leaving only eight parameters. In order to reduce this number further we make the approximation that the true values of A_n^m have the same ratios as those calculated in the point-charge model. By scaling the coefficients A_2^m to A_2^0 and A_4^m to A_4^0 we may reduce the parameters to two. Comparing the best-fit energy levels with the experimental values should enable us to assess the quality of our calculated A_n^m's. The results of such a fitting procedure are given in Table IV. Unfortunately they are not of sufficient quality for one to draw strong conclusions.

In addition to calculations of the type just completed there are other useful methods of regarding the higher configuration spectra. An early attempt to deduce the extent of the $5d$ configuration for each of the rare earths may be found in Dieke's book. The detailed origin of these estimates is not given but they were made using a limited amount of experimental data and some observed regularities in the lanthanide spectra. Figure 14 gives a comparison of our measurements to Dieke's values for the free ion.[31] One would expect that an effect of the crystal field would be to lower the onset of the configuration for each ion. In general this is true though it may not be the case for terbium. More recent efforts of this type have been made by Brewer,[11] Martin,[12] and Sugar and Reader.[13] Their methods are based on the following facts: The energy difference Δ between two configurations differing by a single electron level (e.g., $4f^n$ and $4f^{n-1}5d$) is not a smooth function of atomic number. However the difference between the Δ's for configurations possessing the

TABLE III. Experimental energy levels of the $5d$ configuration of Ce^{3+} in LaF_3 and those calculated from the point-charge model (cm^{-1}).

Theory	Experiment
15 339	7624
4009	1774
3821	−446
−3476	−3226
−19 696	−5776

TABLE IV. Comparison of the fitted crystal-field parameters of cerium with those calculated in the point-charge model. The fitted energy levels are compared with experiment (cm^{-1}).

	Parameters	
	Best fit	Point charge
A_2^0	−322.9	−2060
A_4^0	−40.99	−155.6
	Energy levels	
Theory		Experiment
7947		7614
5010		1774
−2143		−446
−4100		−3226
−7715		−5776

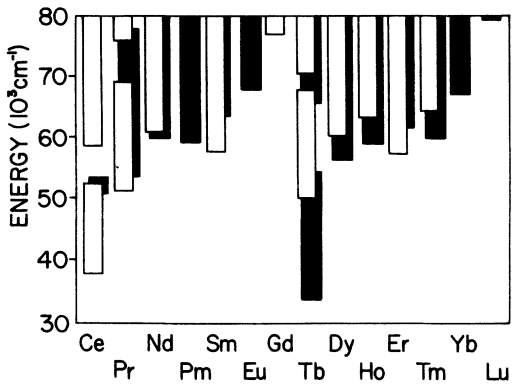

FIG. 14. Comparison of our measurements (white) for the extent of the $5d$ configuration in LaF_3 with the free-ion values (black) projected by Dieke. (See Ref. 28). The $6s$ levels are included for cerium and praseodymium.

same $4f$ core but possessing additional electrons [e.g., $\Delta(4f^n\text{-}4f^{n-1}5d) - \Delta(4f^n 6s\text{-}4f^{n-1}5d6s)$] is a fairly constant value for all the lanthanides. This allows the combination of data from free-ion spectra at different stages of ionization. Brewer used this to estimate the energy of the lowest state of many rare-earth configurations beginning with measured energies for neutral rare earths. Martin estimated the $4f^n - 4f^{n-1}5d$ energy difference (measured between the lowest levels of the configuration) for neutral, monovalent, and divalent ions from a few measured values. Sugar and Reader applied the principle to estimate trivalent ion energy differences using Martin's results. Table V presents a comparison of our measured value for the $5d$ absorption onset in LaF_3 to Loh's[39] measurement in CaF_2 and Sugar and Reader's free-ion band beginning. As expected one sees in general a lowering of the onset caused by the crystal field.

One other empirical point should be mentioned. Loh reports some success in fitting his data with states generated by superimposing the energy levels of the $4f^{n-1}$ core on the two states formed by the crystal field acting on the $5d$ electron.[14] The site symmetry of LaF_3 is such that it splits the $5d$ state into more than just two energy levels making our spectra too complicated for Loh's analysis. However, the case of terbium may be an exception. The $4f^{n-1}$ core for terbium is analogous to the gadolinium $4f^n$ configuration which consists of a ground state more than 30 000 cm^{-1} below the next higher state. This means that the structure of the terbium spectrum should arise entirely from the $5d$ electron split by the field. The clearly resolved structure observed in the terbium trace does imply a small number of lines arising from the crystal field operating on the ^7D and ^9D levels formed from the $5d$ electron and the ^8S core.

TABLE V. Comparison of the band bottom for the free ions with the $4f - 5d$ absorption onset for ions in LaF_3 and CaF_2. The free values are from Ref. 10; the CaF_2 from Loh, Ref. 39.

Ion	Free	LaF_3	CaF_2
Ce	49 737	37 800	32 500
Pr	61 171	51 300	45 600
Nd	70 100	60 600	55 900
Pm	73 300		
Sm	73 700	57 700	59 500
Eu	81 800		68 500
Gd	91 200	77 000	>78 000
Tb	54 900	50 000	46 500
Dy	66 300	60 300	58 900
Ho	74 200	63 300	64 100
Er	75 400	57 500	64 200
Tm	74 300	64 500	64 000
Yb	80 200		70 700
Lu	90 433		>80 000

VI. CONCLUSION

We have presented a rather exhaustive study of the vacuum uv absorptions of trivalent lanthanide ions in LaF_3. Although it appears that the choice of LaF_3 as a host material makes theoretical calculation for comparison with experiment unrewarding: the data may prove amenable to empirical analysis. It is our hope that the research may lead to new solid-state lasers operating in the uv. Several possibilities of this sort suggest themselves. Plans for future work in this area include investigation of different host materials, a study of actinide series ions, and some time-resolved studies.[40]

ACKNOWLEDGMENT

We wish to express our appreciation to the staff of the University of Wisconsin Physical Science Laboratory for their assistance in making these measurements.

†Work supported by the Air Force Office of Scientific Research under Grant No. AFOSR-70-1953, Project No. 9763. Physical Sciences Laboratory work supported by the AFOSR under Contract No. F44-620-C-0029.

*Present address: Department of Chemistry, University of Maryland, College Park, Md. 20742.

‡Present address: Department of Physics, Stanford University, Stanford, Calif. 94305.

[1]J. C. Slater, Phys. Rev. 34, 1293 (1929).
[2]G. Racah, Phys. Rev. 61, 186 (1942).
[3]G. Racah, Phys. Rev. 62, 438 (1942).
[4]G. Racah, Phys. Rev. 63, 367 (1943).
[5]W. G. Harter, Phys. Rev. A 8, 2819 (1973).
[6]B. R. Judd, Phys. Rev. 125, 613 (1962).
[7]B. G. Wybourne, J. Opt. Soc. Am. 55, 928 (1965).
[8]Leo J. Brewer, J. Opt. Soc. Am. 61, 1660 (1971).
[9]W. C. Martin, J. Opt. Soc. Am. 61, 1682 (1971).
[10]Jack Sugar and Joseph Reader, J. Chem. Phys. 59, 2083 (1973).
[11]L. R. Elias, R. Flach, and W. M. Yen, Appl. Opt. 12, 138 (1973).
[12]R. J. Lang, Can. J. Res. A 14, 127 (1935).
[13]R. A. Buchanan, H. E. Rast, and H. H. Caspars, J. Chem. Phys. 44, 4063 (1966).
[14]Eugene Loh, Phys. Rev. 154, 270 (1967).
[15]W. J. Manthey, Phys. Rev. B 8, 4086 (1973).
[16]T. Szezurek, G. W. F. Drake, and M. Schlesinger, Phys. Rev. B 8, 4910 (1973).
[17]L. R. Elias, W. S. Heaps, and W. M. Yen, Phys. Rev. B 8, 4989 (1973).
[18]A. Zalkin, D. H. Templeton, and J. E. Hopkins, J. Inorg. Chem. (Jerus.) 1466 (1966).
[19]H. M. Crosswhite, G. H. Dieke, and Wm. J. Carter, J. Chem. Phys. 43, 6 (1965); 43, 2047 (1965).
[20]Jack Sugar, J. Opt. Soc. Am. 61, 727 (1971).
[21]W. T. Carnall, P. R. Fields, and R. Sarup, J. Chem. Phys. 51, 61 (1969); 51, 2587 (1969).
[22]H. H. Caspars, H. E. Rast, and R. A. Buchanan, J. Chem. Phys. 42, 3214 (1965).
[23]M. J. Weber (private communication).
[24]Wolfgang Baer, John G. Conway, and Sumner P. Davis, J. Chem. Phys. 59, 5 (1973); 59, 2294 (1973).
[25]H. E. Rast, J. L. Fry, and H. H. Caspars, J. Chem. Phys. 46, 4 (1967); 46, 1460 (1967).
[26]W. T. Carnall, P. R. Fields, and R. Sarup, J. Chem. Phys. 54, 4 (1971); 54, 1476 (1971).
[27]J. F. Kielkopf and H. M. Crosswhite, J. Opt. Soc. Am. 60, 347 (1970).
[28]G. H. Dieke, in *Spectra and Energy Levels of Rare Earth Ions in Crystals*, edited by H. M. Crosswhite and Hannah Crosswhite (Wiley, New York, 1968), p. 54.
[29]J. L. Fry, H. H. Caspars, H. E. Rast, and S. A. Miller, J. Chem. Phys. 48, 2342 (1968).
[30]J. L. Fry, H. H. Caspars, and H. E. Rast, J. Chem. Phys. 53, 8 (1970); 53, 3208 (1970).
[31]G. H. Dieke and S. Singh, J. Chem. Phys. 35, 555 (1961).
[32]F. Varsanyi and G. H. Dieke, J. Chem. Phys. 36, 835 (1962).
[33]F. Varsanyi and G. H. Dieke, J. Chem. Phys. 36, 2951 (1962).
[34]William F. Krupke and John B. Gruber, J. Chem. Phys. 41, 5 (1964); 41, 1225 (1964).
[35]W. T. Carnall, P. R. Fields, J. Morrison, and R. Sarup, J. Chem. Phys. 52, 8 (1970); 52, 4054 (1970).
[36]J. Sugar and V. Kaufman, J. Opt. Soc. Am. 62, 562 (1972).
[37]It recently has been called to our attention that S. Matties and D. Welsch [Phys. Status Solidi B 68, 125 (1975)] have used a more sophisticated point-charge model developed by D. J. Newman [Adv. Phys. 20, 197 (1971)] which takes account of many electron effects as well as the electrostatic contributions to the crystal-field parameters. The authors cited calculated these parameters for the $(4f)^2$ Pr^{3+} configuration. Here there are enough lines to obtain a least-squares fit for all required parameters. In any event, this more sophisticated treatment does not lead to very good agreement with experimental results either. In comparing these results with those presented in this paper, transformations in reference coordinates and the A parameters must be made.
[38]J. S. Griffith, *The Theory of Transition Metal Ions* (Cambridge University, Cambridge, 1961), p. 104.
[39]Eugene Loh, Phys. Rev. B 4, 6 (1971); 4, 2002 (1971).
[40]W. S. Heaps, D. S. Hamilton, and W. M. Yen, Opt. Commun. 9, 3 (1973); 9, 304 (1973).